

Porous Mullite Ceramics Formed by Direct Consolidation Using Native and Granular Cold-Water-Soluble Starches

Mariano H. Talou,^{‡,†} Rodrigo Moreno,[§] and M. Andrea Camerucci[‡]

[‡]Ceramics Division, Research Institute for Materials Science and Technology (INTEMA), CONICET/UNMdP, B7608FDQ Mar del Plata, Argentina

[§]Institute of Ceramics and Glass (ICV), CSIC, 28049 Madrid, Spain

In this article, the processing and microstructures of porous mullite bodies prepared by modifying the conventional route of the starch consolidation casting method were studied. The proposed route, called the “soluble route”, involves the use of native starches (i.e., potato, cassava, and corn starches) and a synthesized granular cold-water-soluble (GCWS) starch. Stable aqueous mullite-starch suspensions (0.25 starch volume fraction of 40 vol% total solids) were prepared by mixing. The total starch content was a mixture of ungelatinized native starch and GCWS starch with a 1:10 ratio of GCWS starch to total starch. Steady-state shear flow properties of the suspensions were analyzed by measuring viscosity. The addition of GCWS starch increased the starting suspension viscosity and thus prevented the particle segregation. Porous mullite bodies were obtained by heating (80°C, 2 h) the suspensions in metallic molds and by drying (40°C, 24 h) and sintering (1650°C, 2 h) the green disks after burning out the starch (650°C, 2 h). Green bodies obtained before and after the burning-out process, and the sintered disks were characterized with density and porosity measurements (Archimedes method) and microstructural analysis by SEM. The phases generated after the sintering process were determined by XRD analysis, and pore size distributions were studied by Hg-porosimetry. The obtained results showed that the use of the GCWS starch made the shaping of homogeneous mullite bodies without cracks or deformations possible along with the development of controlled porous microstructures.

I. Introduction

Porous ceramics possess various specific properties: low density, low specific heat, low thermal conductivity, high surface area, and high permeability. Materials with such properties can be used in a wide range of technological applications ranging from catalyst supports, bioceramics, filters, combustion burners, among others. In particular, porous mullite ($3\text{Al}_2\text{O}_3 \cdot 2\text{SiO}_2$) materials can be used as thermal insulators because of their low thermal expansion coefficient and thermal conductivity and their good mechanical properties at high temperature.^{1–4}

Among the direct consolidation methods of ceramic suspensions, techniques in which gelling compounds are used as body-forming and pore-forming agents have become one of the most popular processing routes of porous ceramics. Thus, the starch, which can be used as a consolidating agent of the ceramic suspension when the system is heated between 50°C

and 85°C and as a pore former at high temperature after burning, constitutes the basis of a noncontaminating low-cost consolidation technique called “starch consolidation casting” (SCC).^{5,6} In this method, when the aqueous ceramic-starch suspension is heated, the starch granules swell by water absorption, decreasing the available free water. The ceramic particles (usually of lower size than the starch granules) are thus pressed together in the interstitial space to consolidate into a solid body.

Pabst *et al.*⁷ proposed a model for ceramic body formation that involves two steps: first, the drainage of the excess water by swelling starch granules, and second, the forming of a rigid network of gelatinized starch components that extend into the interstices among the ceramic particles before transformation into a viscoelastic gel, with a subsequent viscosity increase. After calcination and sintering treatments, a porous material is obtained. The porosity thus generated is associated mainly with highly interconnected open pores and depends on the amount, shape, and size of the swollen starch granules.

In the first reported investigations about this forming method,^{5,6} the use of native starches as a body-forming agent was not recommended because highly deformed green bodies were obtained. Furthermore, the most satisfactory results were achieved when chemically modified starches were used, in particular an etherified potato starch modified by hydroxyl-propylation and cross-linking (i.e., TRECOMEX AET1). In these cases, chemical modification is the factor that determines the faster water uptake due to the more open starch granule structure. On the basis of the problems associated with using native starches in ceramic forming by direct consolidation, we have recently reported some modifications to the conventional method.^{8,9}

Nevertheless, native starches can also be physically modified. Synthesized granular cold-water-soluble (GCWS) starches are physically modified starches characterized by a change in the supramolecular order that does not damage its granular shape. Their granules have the ability to instantly swell in water at room temperature, which produces suspensions with viscosities higher than their native counterparts or similar to those of the native starch suspensions after heating.¹⁰ In addition, GCWS starches provide gels with greater strength than the pregelatinized traditional starches obtained by roll drying, spray drying, or extrusion.^{11,12} In spite of these advantages, however, the use of this modified starch type for the preparation of porous ceramics using the SCC technique has not been reported up to now.

GCWS starches can be prepared by several methods: (a) treating a slurry of native starch and a monohydric alcohol with an alkaline solution;¹³ (b) heating starch in aqueous monohydric alcohol solutions at 150°C–170°C under elevated pressure;¹⁴ and (c) heating native starch in aqueous polyhydric alcohol (e.g., 1,2-propanediol) solution at approximately 115°C at atmospheric pressure.^{10,11} The cold-water swelling

G. Franks—contributing editor

Manuscript No. 34005. Received October 22, 2013; approved January 21, 2014.

[†]Author to whom correspondence should be addressed. e-mail: mtalou@fi.mdp.edu.ar

of these starches has been attributed to the conversion of the native double-helical crystalline domains of amylose and amylopectin side-chains (A-, B-, or C-type polymorphs) into a weak single helix crystalline structure (V-type) or an amorphous structure, whereas the granular integrity of the starch is preserved. Removal of alcohol by drying leaves an empty cavity in the center of the helices, which results in starch granules that are metastable and cold-water-soluble.^{12,13,15,16}

In this study, a new forming route of aqueous mullite-native starch suspensions, alternative to conventional route, was designed with the aim to develop green bodies without deformation and with homogeneous porous microstructures. Taking this into account, it was considered that an increase in the suspension viscosity could be produced to achieve such characteristics and thereby minimize the possible segregation of mullite particles and starch granules. Thus, the proposed new processing route, called “soluble route” (SR), involves using a ceramic suspension with native starches and a small amount of a GCWS starch which ought to act as a thickener of the suspension at room temperature before thermal consolidation. The fact of using a thickener with the same chemical nature as starch prevents competition with the dispersant for the adsorption sites of the ceramic particles and in consequence, prevents a change in the stabilization of the suspension.

II. Experimental Procedure

(1) Raw Materials

A high-purity commercial mullite powder (MULS, Baikowski, France) was used as the ceramic raw material. The weight percentages of the main elements (expressed in oxides) were determined by inductively coupled plasma atomic emission spectroscopy (ICP-AES). The alkaline impurity level was less than 0.2 wt%. Excess alumina (even considering that the totality of the determined silica is part of the mullite) with respect to the stoichiometric composition ($\text{Al}_2\text{O}_3 = 71.8 \text{ wt}\%$, $\text{SiO}_2 = 28.2 \text{ wt}\%$) was identified. Mullite 3/2 (JCPDS File 74-2419) as primary phase, and α -alumina (JCPDS File 82-1399), θ -alumina (JCPDS File 11-0517), and cristobalite (JCPDS File 77-1317) as secondary phases, were identified by XRD (X’Pert PRO, PANalytical, radiation of CuK_α at 40 mA and 40 kV). In addition, a low-intensity band was also observed in the zone of the more intense diffraction peaks of silica polymorphs ($20\text{--}30^\circ 2\theta$), which is associated with non-crystalline silicate phases. The powder density (3.07 g/cm^3) was measured by He-pycnometry (Multipycnometer, Quantachrome Co.). This value was lower than theoretical densities of mullite (3.16 g/cm^3), α - Al_2O_3 (3.98 g/cm^3), and θ -alumina (3.28 g/cm^3) due to the contribution of cristobalite (2.3 g/cm^3) and noncrystalline silicate phases ($\sim 2.2 \text{ g/cm}^3$). On the other hand, the mullite powder presented a medium crystallinity that was associated in part with the presence of small narrow- and medium-height diffraction peaks compared with the characteristic peaks of diffractograms of highly crystalline commercial mullite powders.¹⁷ Taking into account these results, it can be inferred that the commercial mullite powder comes from a synthesis process in which the total conversion of the starting mixture (ammonium alum and silica) was not achieved.¹⁸ The mullite powder presented a bimodal particle size distribution (Mastersizer S; Malvern Ltd., UK) with a low mean volume diameter ($D_{50} = 1.5 \mu\text{m}$), a high volume percentage ($\sim 30\%$) of fine particles $< 1 \mu\text{m}$, and contained agglomerates up to $50 \mu\text{m}$ in size due to the presence of the very fine particles. These results are consistent with the high value of the specific surface area ($13.5 \text{ m}^2/\text{g}$) determined by the BET method (Monosorb, Quantachrome Co.). Moreover, it was previously determined⁸ that the mullite powder consists of very small three-dimensional particles, some of them faceted, with equiaxial morphology, as well as agglomerates of the smallest particles, which is in agreement with the granulometric distribution.

Commercial native starches (Avebe S.A., Argentina)⁸ derived from cassava, corn, and potato (Table I), were also used as raw materials. Real densities and total lipid content were determined by He-pycnometry (Multipycnometer, Quantachrome Co.) and Soxhlet extraction method (IRAM 15040), respectively. The values obtained for these parameters were in the range of the values reported for these starch types.¹⁹ In addition, the crystalline molecular order within the starch granules was analyzed by XRD (X’Pert PRO, PANalytical). Based on peak positions, the cassava and corn starches were identified as A-type (15.2 , 17.1 , 18.0 , and $22.9^\circ 2\theta$), whereas the potato starch was identified as B-type (5.4 , 15.0 , 17.2 , 21.8 , 24.0 , and $17.2^\circ 2\theta$). Moreover, the degree of crystallinity for the starches (cassava = 32%, corn = 31% corn, potato = 25%) was quantitatively calculated from the ratio of the area of all peaks to the total area. The particle size distributions were analyzed (Mastersizer S, Malvern Ltd.) using stabilized aqueous starch suspensions. The three starches presented bimodal granulometric distributions, with a low volume percentage ($< 5\%$) of small granules, which can be linked to impurities or broken granules. The moisture weight percentage was determined by thermogravimetric analysis, TGA (Shimadzu TGA-50, Japan) at $10^\circ\text{C}/\text{min}$ up to 700°C , in air. Starch transition temperatures were determined by DSC (Shimadzu DSC-50, Japan) at $5^\circ\text{C}/\text{min}$ up to 120°C . The granule morphology analysis of the dry starches was performed by SEM (Jeol JSM-6460, Japan).¹² Potato starch exhibited the largest granules, with smooth surfaces and oval or spherical forms. Corn and cassava starches presented granules with polyhedral form, but the corn starch granules were most representative of this type.

(2) Processing and Characterization of Prefired Mullite Bodies

(A) *Preparation and Characterization of Granular Cold-Water-Soluble Starch:* The GCWS starch was prepared by heating an aqueous native cassava starch suspension and 1,2-propanediol to 114°C , followed by solvent exchange with ethanol.^{10,12} Their cold-water solubility and viscosity in aqueous media at room temperature were the parameters taken into account to select the native starch employed to synthesize the GCWS starch. Among different native starches studied for the cold-water-soluble starch preparation, the GCWS cassava starch exhibited the highest cold-water solubility ($92\text{--}99\%$) and the viscosity of its aqueous suspension at room temperature was similar to the native cassava starch after heating.¹⁰ The optimal concentration of GCWS starch in the total starch content used to form disks by the proposed processing route (SR) was previously determined²⁰ based on apparent viscosity measurements of aqueous mullite-starch suspensions with different amounts of the selected GCWS starch. The crystalline molecular arrangement within the starch granules and their degree of crystallinity were analyzed by XRD using the same experimental conditions used in the native starch tests. In addition, the morphology of the dried GCWS starch granules was analyzed by SEM, and the granule size distribution was determined by laser diffraction using water as the liquid medium of the suspension. The behavior of their aqueous suspensions as a function of temperature ($30^\circ\text{C}\text{--}85^\circ\text{C}$) was evaluated from the analysis of the images captured using transmission optical microscopy (Leica DMLB, Germany) with a hot stage (Linkam THMS 600, UK) and a video camera (Leica DC 100, Germany).^{13,14}

(B) *Shear Flow Properties of Aqueous Mullite-Starch Suspensions:* Based on previously selected experimental conditions,^{20,21} aqueous mullite-starch suspensions (40 vol% total solid loading) were prepared by: (a) mixing mullite powder in water to a solid content of 40 vol% dispersing with 0.45 wt% Dolapix CE-64 (Zschimmer & Schwarz, Germany) with respect to the powder amount; (b) homogenizing in a ball mill for 6 h; and (c) adding and mixing for

Table I. Characteristics of the Commercial Native Starches

Starch	ρ_r (g/cm ³)	Moisture content (wt%)	Lipid content (wt%)	T_p (°C)	D_{50} (μm)
Cassava	1.49	11.5	0.99	67.5	13.6
Corn	1.49	10.9	1.63	66.8	14.8
Potato	1.47	14.4	0.37	65.0	47.8

ρ_r : real density, T_p : endothermic peak temperature, D_{50} : mean volume diameter.

5 min a volume of aqueous starch suspension (40 vol%) to obtain starch and mullite final contents of 10 vol% and 30 vol%, respectively. The total starch content was a mixture of cassava, corn, or potato starches with the GCWS starch prepared from native cassava starch in such way that the ratio of GCWS to total starches was 1:10.

The shear flow properties of aqueous mullite-starch suspensions with and without GCWS starch were analyzed from viscosity measurements (rheometer Haake RS50; Thermo Electron Corp., Germany) using a double-cone/plate sensor configuration (DC60/2°, Thermo Haake, Germany). Flow curves were obtained with a three-stage measuring program with a linear increase in shear rate from 0 to 1000 s⁻¹ in 300 s, 60 s at 1000 s⁻¹, and a further decreasing to zero shear rate in 300 s.

(C) *Forming- and Burning-Out Processes*: Mullite-starch green disks (labeled as SR_{bb}) were formed by pouring the aqueous mullite-starch suspension at room temperature into stainless steel cylindrical molds (diameter = 2.20 cm; height = 1.00 cm) and heating them in an electric stove (Memmert UFP 400, Germany) at 80°C for 2 h. Once the consolidation was finished, the samples were taken out of their molds and dried at 40°C for 24 h.

Burned mullite bodies (labeled as SR_{ab}) were obtained by burning out the starch at a heating rate of 1°C/min up to 650°C for 2 h in an electric furnace with SiC heater elements. The calcining temperature was selected based on the results obtained from TGA tests (Shimadzu TGA-50, at 10°C/min up to 700°C, in air) of starches used as raw materials (native and GCWS starches). This temperature was considered the temperature at which all the organic components (starches and organic additives) were completely removed. Furthermore, to evaluate the effective removal of the starch from the green compacts by the burning-out process, thermogravimetric tests were performed on mullite-starch (1°C/min up to 650°C, 2 h) and burned samples (10°C/min up to 700°C). In all the TGA tests, a very low heating rate (1°C/min) was used to minimize the generation of defects in the green bodies or their rupture during the burnout process due to the evolution of a high volume of gas (particularly water vapor and carbon dioxide) caused mainly by the oxidative degradation of the starch.

From the TGA tests of starch samples, the following percent weight losses were determined: 12.7 wt% up to 150°C, which is attributed to the removal of the water physically adsorbed onto the surface of the starch granules; 61.2 wt% between 250°C and 350°C and 26.1 wt% in the range 350°C–550°C, which was associated with the elimination of starch by thermal and oxidative degradation of the polymeric chains of its structure. After 550°C, no additional weight loss was registered. Therefore, a temperature of at least 600°C was required to remove the starch completely. With regard to the TGA tests of mullite-starch samples, the percent weight losses registered for cassava, corn, and potato starches—assuming that all the organic dispersant was completely removed—were 11.9, 12.9, and 9.3%, respectively. Taking into account these values and considering the initial amount of each starch in the green samples and the associated experimental error, it was assumed that all the starch present in the green samples was completely removed during the burning process.

Densities (ρ) of the disks obtained before (SR_{bb}) and after (SR_{ab}) the burning-out process were determined by immersion in Hg, and porosities (% P) were calculated from $100 \cdot (1 - \rho/\rho_p)$. For SR_{bb}, ρ_p was the density of the powdered mixture of mullite and starch determined by He-pycnometry. For SR_{ab}, ρ_p was the pycnometric density value of the mullite powder. The microstructural analysis of the green materials was performed by SEM on fracture surfaces of the disks.

(3) Sintering and Characterization of Porous Mullite Bodies

Porous mullite bodies were finally prepared by sintering at 1650°C for 2 h in an electric furnace with MoSi₂ heater elements (Carbolite RHF 17/6S; Carbolite Ltd., England). Samples were heated up to the sintering temperature at 5°C/min and subsequently cooled until room temperature at 5°C/min.

The phases generated after the sintering process were identified by XRD analysis (X'Pert PRO, PANalytical, radiation of CuK_α at 40 mA and 40 kV). Bulk densities (ρ_s) and open porosities (% P_o) were determined by the Archimedes method in water, taking into account an error equal to the Hg-immersion method. Total porosities (% P_s) were calculated from $100 \cdot (1 - \rho_s/\rho_{ps})$, where ρ_{ps} was the density of the powdered sample treated at 1650°C for 2 h, determined by He-pycnometry. From both values, % P_o and % P_s , closed porosities (% P_c) were obtained. In addition, the linear and volumetric shrinkage of sintered samples were calculated by using disk geometrical dimensions measured with a slide caliper. The final microstructures were analyzed by SEM on fracture surfaces of disks. The mean size and morphology of the cavities and the grains were determined together with the degree of pore connectivity (defined as the open porosity/total porosity ratio). Mercury porosimetry (AutoPore II 215; Micromeritics) was used to determine the pore throat size distributions.

III. Results and Discussion

(1) Properties of Granular Cold-Water-Soluble Starch

Granular cold-water-soluble (S cassava starch showed a V-type X-ray diffraction pattern (13.0 and 19.9°2 θ)²² and a rather lesser degree of crystallinity (18%) than its native counterpart (32%) (Fig. 1). The single-chain conformation can give either an amorphous X-ray pattern indicative of a random arrangement of polymer chains or the V-type X-ray pattern that is due to crystals of single-helical chains. Rajagopalan and Seib¹⁵ reported that the X-ray diffraction pattern of the treated starches was amorphous immediately after heating the starches in aqueous polyhydric alcohol, whereas the diffraction pattern changed to a V-type pattern after the solvent (aqueous polyhydric alcohol) exchange with ethanol was produced. Several authors proposed a mechanism in which the starch molecules (amylose and amylopectin) may form single-helical complexes (V-complex) with ethanol molecules during solvent exchange after the double-helical structure of native starch is dissociated by heating in aqueous 1,2-propanediol.^{13,15,16} Removal of alcohol by drying leaves the starch in a metastable state and soluble in cold water.

SEM images of the GCWS cassava starch together with a SEM image of native cassava starch are shown in Fig. 2. Based on the analysis performed, the majority of granules

suffered some modification to their original morphology, and only a few of them remained intact. Moreover, based on the particle size distribution, the mean size of cold-soluble starch granules ($D_{50} = 29.6 \mu\text{m}$) was rather greater than those of the dry original native granules and similar to those corresponding to the native granules gelatinized at 63°C . It is worth noting that during the preparation treatment of the GCWS cassava starch, the granules could have experienced degradation, hydration, swelling, and loss of crystallinity. These changes are responsible, in part, for the modifications that occur in the granule morphology.²³ In addition, it has been reported that the specific method used to prepare the cold-soluble starches determines the morphology of their granules. The dependence of the characteristics of cold-soluble starch granules on the type of native starch has also been reported.^{11,23} In general, the surface of the obtained GCWS starch granules presented a rough appearance very different from that of the native cassava starch granules in which their surfaces were smooth and without pores. In addition, some of the GCWS starch granules showed internal fragmentation [Fig. 2(c)]; some of the granules even ruptured from the surface; in these cases, remains of material leached from the granule and adhered to their surface could also be observed [Fig. 2(b)]. These facts (changes in the morphology and size of granules) clearly indicate swelling and shrinkage in the internal region of the granule, whereas the thin shell at the granules surface denotes little or no swelling in this region. The lack of swelling in the thin shell is consistent with the “leathery” texture at the granules’ surface. In a few cases [Fig. 2(c)], the occurrence of significant internal shrinkage in a very localized region together with the generation of a resistant shell could have also formed a cold-soluble starch granule with a larger hollow area gave it a donut shape.

Regarding the behavior of aqueous GCWS cassava starch suspensions as a function of temperature (30°C – 85°C)

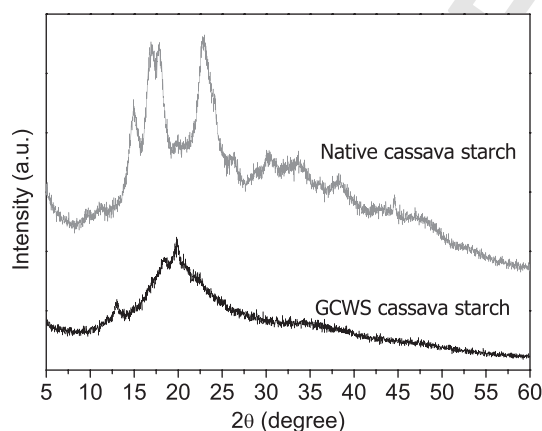


Fig. 1. X-ray diffraction diagrams of native and GCWS cassava starches.

(Fig. 3), even though at 30°C the majority of cold-soluble starch granules had already evidenced some change in their morphology and had become deformed or fragmented, the few granules that remained intact started swelling after 63°C (onset temperature of gelatinization, $T_{G'0}$, of the majority of native cassava starch granules).²⁴ This behavior was notably different to that observed in the aqueous suspension of the native cassava starch (the images of this starch were also included in Fig. 3 for comparative purposes). In this case, the native granules did not grow before reaching the onset temperature of gelatinization (63°C). At temperatures above $T_{G'0}$, a large amount of granules increased in size, up to approximately $40 \mu\text{m}$, and some of them even became deformed and fragmented. A similar behavior was also observed in heated aqueous suspensions of corn and potato native starches.^{20,24} As for the GCWS starch, measuring the diameter of the majority of granules was not feasible because of their very complex morphology. In both systems (native and GCWS starch suspensions) after heating, a mixture of granules or their remains were immersed in a colloidal dispersion of starch components.

Based on these results, it can be assumed that the thermal consolidation process of the ceramic suspension is only controlled by gelatinization of the native starch. The GCWS starch acts as gelling agent (thickener) at room temperature, and because of the low amount added, it only contributes to increasing the viscosity of the ceramic suspension.

(2) Rheological Behavior of Aqueous Mullite-Starch Suspensions

Curves of apparent viscosity as a function of the shear rate of aqueous mullite-starch (cassava, corn, or potato) suspensions with and without added of GCWS starch are shown in Fig. 4. For comparative purposes, the flow curve of an aqueous mullite suspension was also included. Apparent viscosity values for these suspensions are given in Table II.

Aqueous mullite suspensions with native starches presented a complex-fluid behavior, exhibiting a slight shear-thinning (pseudoplastic) to shear-thickening (dilatant) transition for shear rates close to 300 s^{-1} , low thixotropy ($< 400 \text{ Pa/s}$; the area between the up and down stress-shear rate curves was considered as a measure of this parameter), and a progressive decrease in the viscosity while maintained for 60 s at the highest shear rate (1000 s^{-1}). This rheological behavior has been already reported^{21,25,26} for mullite and mullite-starch suspensions with similar properties. Regarding the mullite-starch suspensions with added GCWS starch, a strong shear-thinning behavior was observed throughout almost the entire shear rate range. Moreover, the apparent viscosity values determined at highest shear rates did not substantially modify. However, for these suspensions, higher thixotropy values ($\sim 3500 \text{ Pa/s}$) were determined. In these systems, the registered global rheological behavior can be associated with two overlapped single non-Newtonian behaviors: one corresponds to ceramic suspension with native starch,

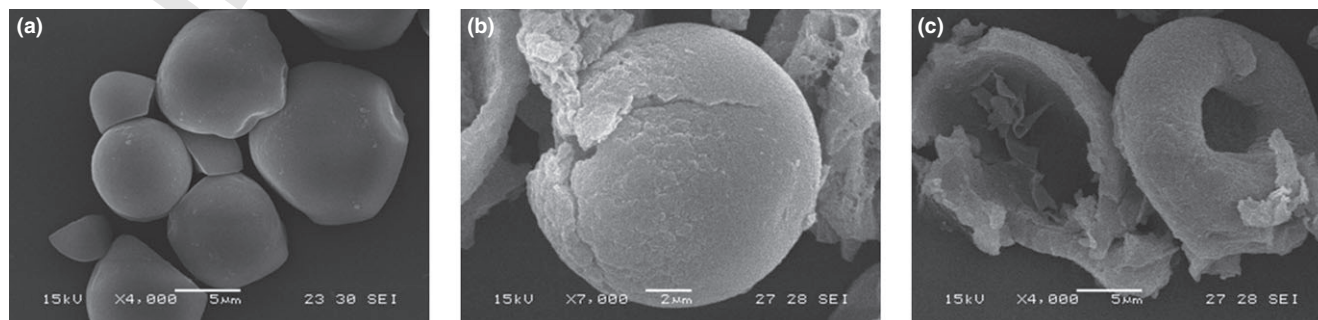


Fig. 2. SEM micrographs of native (a) and GCWS (b and c) cassava starches.

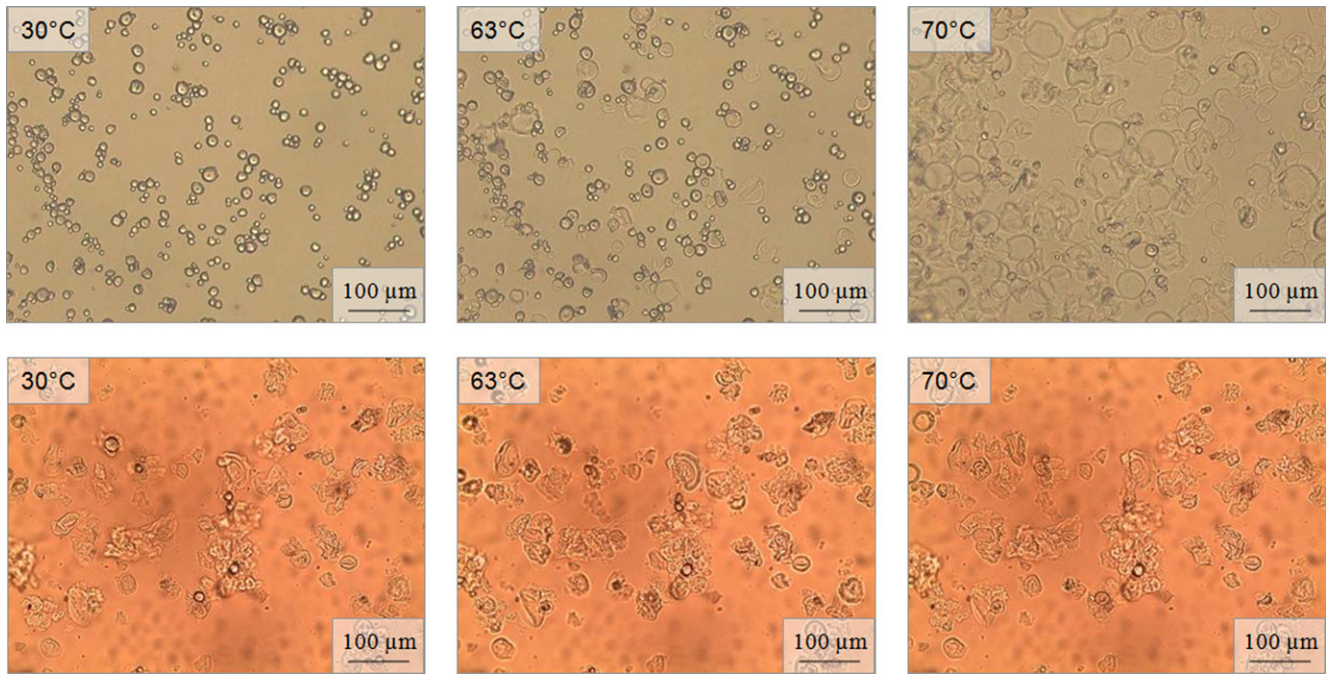


Fig. 3. Optical micrographs of native (top) and GCWS (bottom) cassava starch suspensions heated at different temperatures.

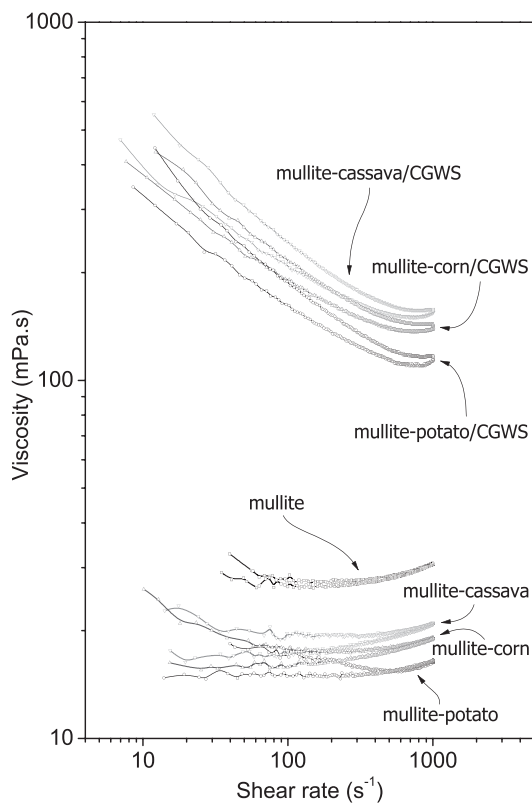


Fig. 4. Viscosity curve for an aqueous mullite suspension and aqueous mullite-starch (cassava, corn, or potato) suspensions with and without GCWS starch.

and the other is associated with the progressive rupture of gel aggregates formed by the GCWS starch, which produces a significant viscosity decrease by increasing the shear rate. In addition, a new gel structure can be partially formed by decreasing the shear rate, which should lead to a higher thixotropy in mullite suspensions with GCWS starch than that of the mullite suspension with only native starch.

The substitution of a small amount of native starch with GCWS starch led to a notable increase in the viscosity (at

least six times higher) of mullite-native starch suspensions, which was related to the ability of GCWS starch granules to instantly swell in water at room temperature. Moreover, the viscosity values obtained when the GCWS starch was used were in the range of the values reported using a chemically modified starch (TRECAMEX AET1) as was reported by Barea *et al.*²⁵ Taking into account that an equal amount of a unique soluble starch was added, the differences registered in the viscosity values for each suspension should be attributed to the role played by each one of the native starches. In fact, the relative order of viscosity obtained was the same as that determined for mullite suspensions with original native starches (mullite-cassava > mullite-corn > mullite-potato).

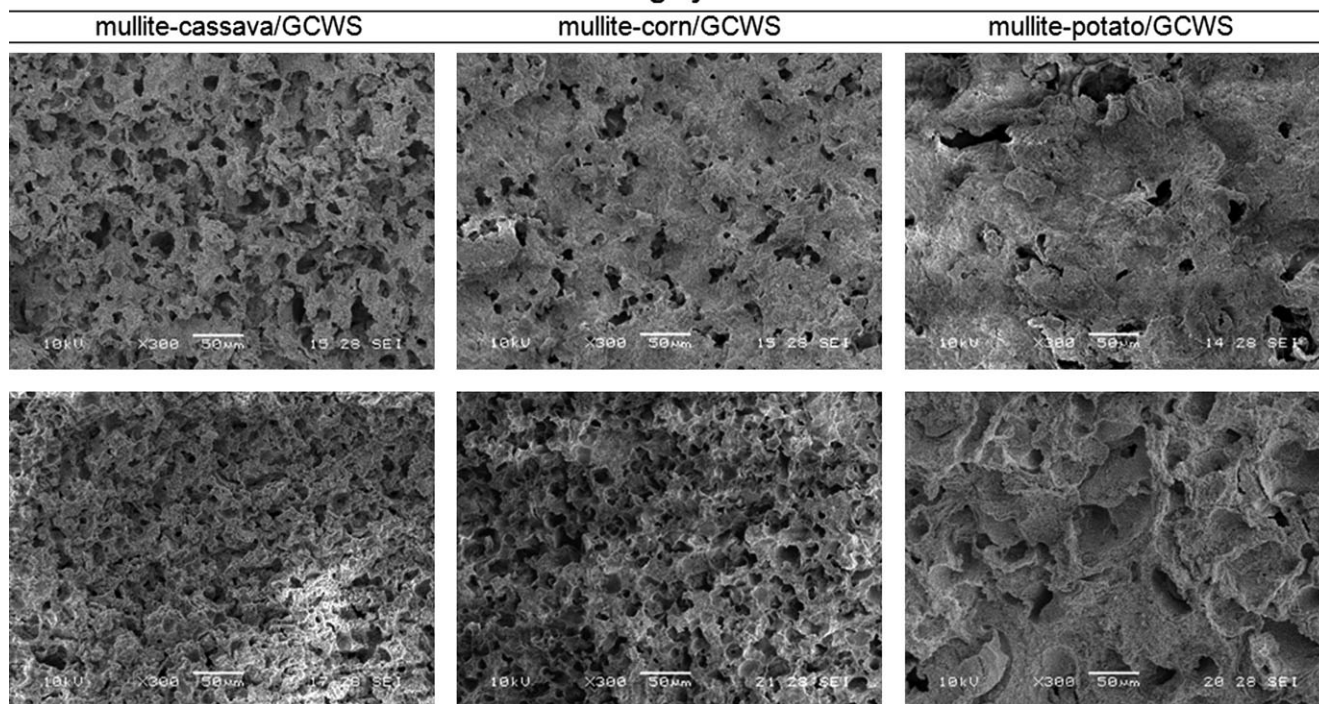
(3) Characterization of Green Bodies

Disks obtained before the burning-out process (SR_{bb}) had a mean diameter of 2.17 ± 0.01 cm and a height of 0.55 ± 0.05 cm, with a shrinkage of 1.3% in diameter and 8.3% in height. Mullite disks obtained after calcination (SR_{ab}) maintained the mentioned dimensions without showing cracks or deformations.

High porosities were achieved in all the green materials. The type of native starch used did not determine significant differences in porosity obtained for disks before calcination ($\%P_{bb} = 56 \pm 1$). On the other hand, the porosity of disks significantly increased after the burn-out process ($\%P_{ab} = 70 \pm 1$) using either of the starches. These values turned out to be consistent with those calculated ($\sim 69\%$) assuming that the totality of the added starch was removed during the burn-out process. This result indicates that there was no segregation of starch granules and mullite particles. Typical SEM images of the fracture surfaces of materials are shown in Fig. 5. In these images, a homogeneous distribution of raw materials can be observed, which confirms that there was no segregation. Moreover, starch granules with integrity were not observed in the green microstructures. This last result can be associated with the occurrence of an advanced gelatinization process that consequently promotes the loss of granular integrity. The advanced gelatinization process and the increase in the initial suspension viscosity related to the presence of the GCWS starch were the determining factors behind the absence of segregation in the green bodies.

Table II. Apparent Viscosities at 1000 s^{-1} (η_{1000}) of Aqueous Mullite-Starch Suspensions

Aqueous suspensions	Mullite content (vol%)	Native starch content (vol%)	GCWS starch content (vol%)	η_{1000} (mPa/s)	Thixotropy (Pa/s)
Mullite-cassava	30	10	0	21	390
Mullite-cassava/GCWS	30	9	1	157	3650
Mullite-corn	30	10	0	19	310
Mullite-corn/GCWS	30	9	1	142	3370
Mullite-potato	30	10	0	16	290
Mullite-potato/GCWS	30	9	1	103	3950

Forming systems**Fig. 5.** SEM micrographs of the fracture surface of disks: SR_{bb} (top) and SR_{ab} (bottom).

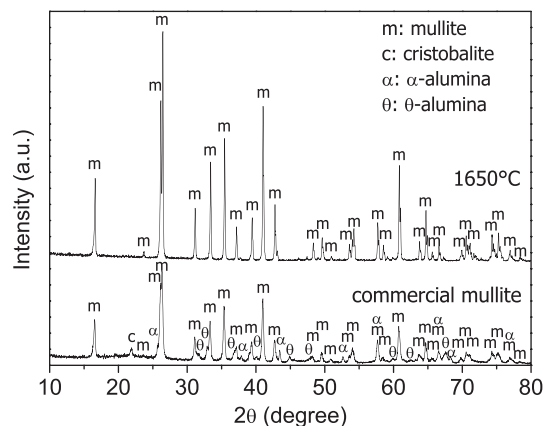
On the other hand, all the materials (Fig. 5) showed similar porosities, in agreement with porosity values determined from density measurements. The porosity of SR_{bb} disks was associated with cavities possessing a high degree of tortuosity throughout the entire thickness of disks, which hindered the accurate measurement of their size. However, it can be observed that in every sample, the cavity sizes correspond to those of the dry starch granules or those with a certain degree of swelling. After the burning-out process, the porosity of materials (SR_{ab}) increased notably, thus maintaining the tortuous morphology of the cavities (Fig. 5).

(4) Characterization of Sintered Porous Mullite Bodies

Mullite 3/2 (JCPDS File 74-2419) was the single crystalline phase present after the sintering process and identified by XRD analysis (Fig. 6). The intensities of the characteristic mullite diffraction peaks were higher than those of the peaks for the as-received mullite powder. On the other hand, the pycnometric density value of the powdered sample (ρ_{ps}) treated at 1650°C was 3.11 g/cm³. Based on these results, it was assumed that a complete mullitization reaction occurred after treatment at 1650°C for 2 h.

Total, open and closed porosity values, together with linear and volumetric shrinkage values of mullite disks obtained after sintering, are given in Table III.

According to the obtained values, the total (43%–46%), open (39%–41%) and closed (3%–5%) porosities of sintered disks were similar for all the native starches used. The

**Fig. 6.** XRD pattern of as-received mullite powder and mullite powder treated at 1650°C, 2 h.

porosity values obtained were in the range of those reported for porous mullite materials prepared by the conventional route with a similar percentage of modified starch.²⁵ It is well-known that total porosities achieved in the materials prepared by SCC do not correspond directly to the nominal starch content in the suspension, but they are significantly higher due to the swelling experienced by the starch granules during the thermal consolidation process. However, despite the fact that swelling capacity depends on the starch type,

the porosity of the disks did not significantly vary with the native starch type, which is the same as what happened in the green bodies and in agreement with the occurrence of a constrained swelling due to steric effects (excluded volume effect).

When the nominal starch content is high, as it was in this study (25 wt%) and as observed in SEM micrographs (Fig. 6), large pores such as convex cavities are in contact or interconnected. In addition, small concave interstitial open pores are present, but some of them close when a sufficient degree of sintering is achieved. Thus, a certain amount of closed pores (Table III) and a high degree of pore connectivity (open porosity/total porosity ratio) was obtained at 1650°C; these parameters were similar for all materials regardless of the native starch used.

As for the linear and volumetric shrinkage of mullite disks, the obtained values were in the range of those reported for bodies consolidated by the conventional route with a waxy corn starch.^{27,28}

Taking into account that the sintering temperature is the main factor determining the matrix porosity and that large pores (bigger than the grain size) embedded in a ceramic matrix with small pores does not contribute significantly to the shrinkage of the body, it can be assumed that the recorded shrinkage in all the mullite disks corresponded essentially to the matrix. Taking into account that for the three native starches the linear and volumetric shrinkage percentages were similar, and assuming that this shrinkage

occurs only in the ceramic matrix, it can be inferred that the packing density of the mullite particles in every green body turned out to be approximately the same. Typical SEM micrographs of porous mullite materials are shown in Fig. 7. Highly magnified images of typical cavities developed with each native starch are shown in Fig. 8.

The large convex cavities (cells) embedded in the mullite matrix were created by the removal of native starch and cold-soluble starch granules (mainly those granules that preserved their integrity or only deformed after swelling process), and much smaller pore channels or throats (window cells) interconnecting these cavities were developed after the sintering treatment. The cavity size was mainly determined by the native starch type, and it was related to dry starch granule sizes or those having suffered some degree of swelling: 10–20 μm for materials prepared with native starches of cassava and corn, and 30–70 μm for those prepared with potato starch. Larger cavities generated from the joining of various cavities were also observed. In particular, many of the cavities formed by removing the potato starch presented a shell and circumferential cracks in the cavity/matrix interface that is separated from the matrix [Fig. 8(c)]. This characteristic was not observed in any of the cavities created by cassava and corn starches. Several authors^{5,6,25} have also reported the formation of these shells and established that they are formed from a certain amount of shrinkage of the starch granule during heating, so that the particles that adhered to the granule are separated from the surrounding

Table III. Total (% P_s), Open (% P_o) and Closed (% P_c) Porosity Values, Degree of Pore Connectivity, and Linear and Volumetric Shrinkage of Sintered Disks

Mullite-native starch system	% P_s	% P_o	% P_c	Pore connectivity degree	Linear shrinkage (%)	Volumetric shrinkage (%)
Cassava	43	39	4	0.9	16.1 \pm 0.9	42 \pm 1
Corn	44	41	3	0.9	15.9 \pm 0.1	41.1 \pm 0.2
Potato	46	41	5	0.9	15.8 \pm 0.9	41 \pm 1

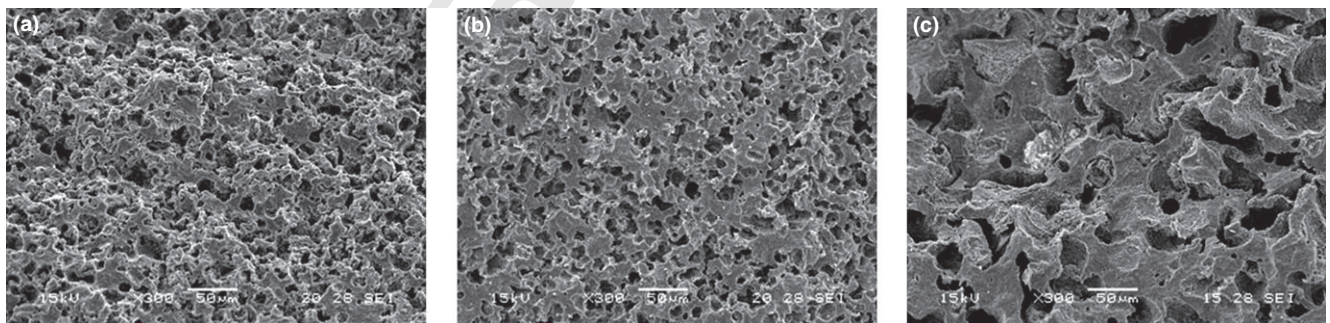


Fig. 7. SEM micrographs of fracture surfaces of sintered disks formed with the GCWS starch and the native starches of cassava (a), corn (b), and potato (c), after sintering at 1650°C.

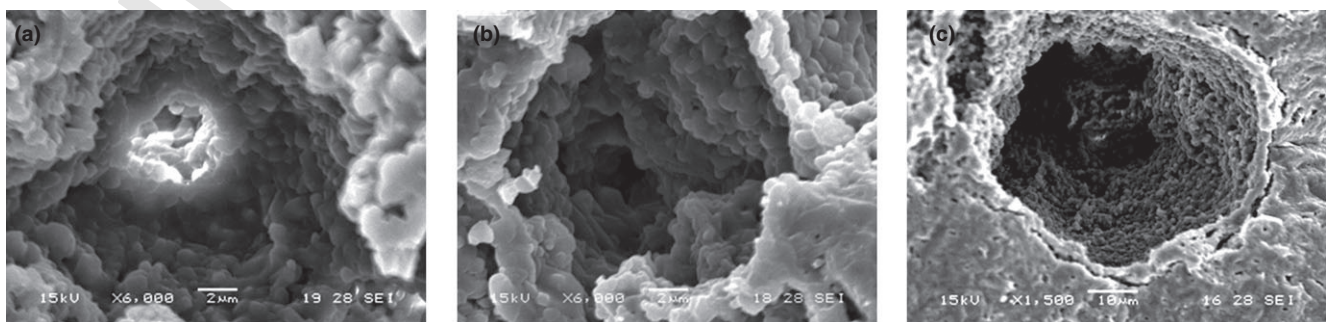


Fig. 8. SEM images of typical cavities developed in materials formed with the starches of cassava (a), corn (b), and potato (c), after sintering at 1650°C.

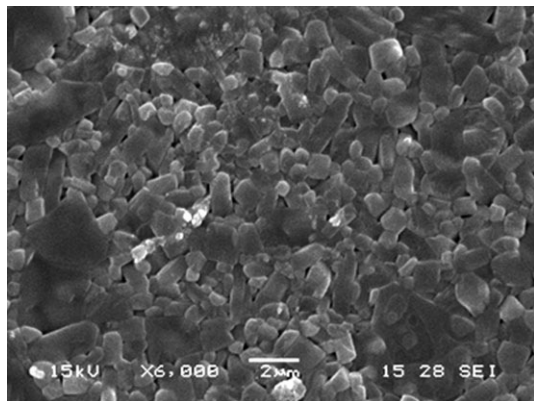


Fig. 9. Typical SEM micrograph of the mullite matrix of a sample sintered at 1650°C.

matrix and remain attached to the starch. Other authors²⁹ have proposed that as many shells as cracks surrounding the cavities could be attributed to a differential shrinkage among regions with different packing density (packing density in the zone adjacent to the cavity is lower than inside it).

The mullite matrix presented a high degree of densification with few small concave pores and submicronic grains (some of them were generated from the mullitization reaction at high temperature), mainly equiaxial ($\sim 0.5 \mu\text{m}$), together with other slightly larger grains with elongated morphology (maximum length and width of $2 \mu\text{m}$ and $0.8 \mu\text{m}$, respectively, and “aspect ratio” < 2.5). The development of elongated grains can be related their growth in presence of liquid phase. Based on these results, it is proposed that the mullite matrix densification was facilitated by the presence of phases based on silicates of low melting point that in turn facilitates the transport of matter, thus increasing the densification rate along with a limited grain growth.

The pore sizes measured in all the materials by mercury porosimetry were much lower than the cavity sizes observed by SEM (Figs. 7 and 8), which was expected based on the characteristics of the developed pores: large cavities interconnected by pore channels or throats of much lower size. This result can be attributed to the “bottle neck” effect that occurs when the mercury accesses inside a large cavity through a narrow channel. In this manner, the pore diameters determined by mercury porosimetry corresponded to the pore throat diameters. According to these results, the pore throat size distributions for all the prepared materials were similar, whereby again there was no significant dependence on the native starch type. The pore throat diameters for the materials prepared with the cassava, corn, and potato starches were in the ranges $3.3\text{--}5.4 \mu\text{m}$, $1.8\text{--}4.9 \mu\text{m}$, and $3.6\text{--}6.3 \mu\text{m}$, respectively. In addition, the pore population corresponding to interstitial pores of much smaller sizes than the cavities was not observed in the total pore size distribution, thus indicating that a high degree of densification of the ceramic matrix occurred during sintering at 1650°C.

The accurate measurement of cavity size by image analysis requires that they are all single and isolated. However, in the porous materials developed by SCC, only interconnected single pores and agglomerates of pores, which could have originated from the rupture of the pore wall or from overlapping or joining of adjacent granules during the forming, are generated by starch removing. As a consequence, the possible overlapping or joining of adjacent granules leads to an overestimated pore size by image analysis. In addition, it is worth noting that if isolated pores appear in a 2D transversal cut, it cannot offer any conclusions as to the pore type in 3D. Mean values and the standard deviation of different parameters such as aspect ratio, and maximum and minimum Feret diameters were obtained by image analysis (Table IV) to

Table IV. Feret Diameters and Aspect Ratios Determined by Images Analysis

Mullite-native starch systems	Aspect ratio	Maximum Feret diameter (μm)	Minimum Feret diameter (μm)
Cassava	1.9 ± 0.7	30 ± 15	18 ± 8
Corn	1.8 ± 0.5	27 ± 10	16 ± 7
Potato	2.0 ± 0.7	77 ± 35	44 ± 20

characterize the size and morphology of the cavities developed in the mullite materials. The aspect ratio refers to the relation between the major and minor axis lengths of the object that were obtained from maximum and minimum Feret diameters. The Feret diameter takes into account the major distance between two parallel tangents of the object to an arbitrary angle.

The large standard deviation values obtained for all the parameters are in agreement with the fact that for preparing these materials, natural pore formers that have a wide granule size distribution, as much in the initial state as after swelling, were mainly used. In addition, the effect of the gelatinization process has should be taken into account. The mean aspect ratio values obtained for all the materials (rather higher than 1, which is the value corresponding to the spherical shape), indicate that the cavity morphology is far from being spherical due to its significant elongation. This parameter was not influenced by the starch type used. However, the native starch type was the determining factor for the Feret diameters. The obtained size range is in agreement with the size range and order estimated from the SEM images. The larger value was obtained for mullite materials prepared with potato starch as well as GCWS cassava starch, whereas the values of the remaining materials were smaller but similar between themselves. In short, homogeneous microstructures with the typical porosity characteristics presented by the ceramic materials prepared by SCC method were developed by adding the GCWS cassava starch in the starting aqueous mullite-native starch suspension.

IV. Conclusions

The presence of a small amount of cold-water-soluble cassava starch in the aqueous mullite suspension with native starch allowed to form homogeneous green mullite bodies without cracks or deformation. This was linked to the increase in the mullite-starch suspension viscosity due to the thickening action of the cold-water-soluble starch prior to the thermal consolidation step process that was almost exclusively controlled by the native starch. The homogeneous microstructures developed by employing the proposed route presented features similar to those shown by porous materials prepared by the conventional route of the SCC method with a similar amount of starch. The high volume porosity achieved was independent of the starch type used and was associated with large, highly interconnected nonspherical cavities whose sizes depended on the starch type and similar pore throats of much less size.

Based on the obtained results, the proposed novel processing route constitutes a potential way to replace the conventional SCC method when native starches are used as consolidator/binder agents, and leads to the development of controlled and homogeneous porous microstructures.

Acknowledgments

The authors gratefully acknowledge Dr. W. Pabst and Msc. E. Gregorová (ICT, Prague, Czech Republic) for measuring the particle size distribution of the synthesized cold-water-soluble starch by laser diffraction. This study was funded by CONICET (Argentina) under project PIP 0936. Dedicated to Prof. Ana L. Cavalieri, an excellent scientist and a better person.

References

- ¹H. Schneider, J. Schreuer, and B. Hildmann, "Structure and Properties of Mullite - A Review," *J. Eur. Ceram. Soc.*, **28** [2] 329–44 (2008).
- ²B. Hildmann and H. Schneider, "Heat Capacity of Mullite - New Data and Evidence for a High-Temperature Phase Transformation," *J. Am. Ceram. Soc.*, **87** [2] 227–34 (2004).
- ³H. Schneider and E. Eberhard, "Thermal Expansion of Mullite," *J. Am. Ceram. Soc.*, **73** [67] 2073–6 (1990).
- ⁴J. H. She and T. Ohji, "Fabrication and Characterization of Highly Porous Mullite Ceramics," *Mater. Chem. Phys.*, **80** [3] 610–4 (2003).
- ⁵O. Lyckfeldt and J. M. F. Ferreira, "Processing of Porous Ceramics by 'Starch Consolidation'," *J. Eur. Ceram. Soc.*, **18** [2] 131–40 (1998).
- ⁶H. M. Alves, G. Tari, A. T. Fonseca, and J. M. F. Ferreira, "Processing of Porous Cordierite Bodies by Starch Consolidation," *Mater. Res. Bull.*, **33** [10] 1439–48 (1998).
- ⁷W. Pabst, E. Týnová, J. Míkač, E. Gregorová, and J. Havrda, "A Model for the Body Formation in Starch Consolidation Casting," *J. Mater. Sci. Lett.*, **21** [14] 1101–3 (2002).
- ⁸M. H. Talou and M. A. Camerucci, "Two Alternative Routes for Starch Consolidation of Mullite Green Bodies," *J. Eur. Ceram. Soc.*, **30** [14] 2881–7 (2010).
- ⁹M. H. Talou, A. G. Tomba Martinez, and M. A. Camerucci, "Green Mechanical Evaluation of Mullite Porous Compacts Prepared by pre-Gelling Starch Consolidation," *Mater. Sci. Eng., A*, **49**, 30–7 (2012).
- ¹⁰S. Rajagopalan and P. A. Seib, "Process for the Preparation of Granular Cold Water-Soluble Starch"; U.S. Patent No. 5,037,929, 1992.
- ¹¹J. Singh and N. Singh, "Studies on the Morphological and Rheological Properties of Granular Cold Water Soluble Corn and Potato Starches," *Food Hydrocolloids*, **17** [1] 63–72 (2003).
- ¹²S. Rajagopalan and P. A. Seib, "Granular Cold-Water-Soluble Starches Prepared at Atmospheric Pressure," *J. Cereal Sci.*, **16** [1] 13–28 (1992).
- ¹³J. Chen and J. Jane, "Properties of Granular Cold-Water-Soluble Starches Prepared by Alcoholic-Alkaline Treatments," *Cereal Chem.*, **71** [6] 623–6 (1994).
- ¹⁴J. E. Eastman and C. O. Moore, "Cold Water Soluble Granular Starch for Gelled Food Compositions"; U.S. Patent No. 4,465,702, 1984.
- ¹⁵S. Rajagopalan and P. A. Seib, "Properties of Granular Cold-Water-Soluble Starches Prepared at Atmospheric Pressure," *J. Cereal Sci.*, **16** [1] 29–40 (1992).
- ¹⁶R. F. Tester, J. Karkalas, and X. Qi, "Starch-Composition, Fine Structure and Architecture," *J. Cereal Sci.*, **39** [2] 151–65 (2004).
- ¹⁷M. A. Camerucci, "Desarrollo y Evaluación de Materiales Cerámicos de Cordierita y Cordierita-Mullita (Development and Evaluation of Cordierite and Cordierite-Mullite Ceramic Materials)"; Ph. D. Thesis, National University of Mar Del Plata, Mar del Plata, 1999.
- ¹⁸R. Wojciechowska, W. Wojciechowski, and J. Kaminski, "Thermal Decompositions of Ammonium and Potassium Alums," *J. Therm. Anal. Calorim.*, **33** [2] 503–9 (1988).
- ¹⁹J. Jane, "Structural Features of Starch Granules II"; Chapter 6 in *Starch: Chemistry and Technology*; Edited by J. N. BeMiller and R. L. Whistler. Academic Press, New York, 2009.
- ²⁰M. H. Talou, "Procesamiento de Materiales Cerámicos Porosos de Mullita por Consolidación Directa con Almidón (Processing of Porous Mullite Ceramics by Starch Direct Consolidation)"; Ph. D. Thesis, National University of Mar Del Plata, Mar del Plata, 2012.
- ²¹M. H. Talou, M. A. Villar, M. A. Camerucci, and R. Moreno, "Rheology of Aqueous Mullite-Starch Suspensions," *J. Eur. Ceram. Soc.*, **31** [9] 1563–71 (2011).
- ²²A. Buleón, P. Colonna, V. Planchot, and S. Ball, "Starch Granules: Structure and Biosynthesis," *Int. J. Biol. Macromol.*, **23** [2] 85–112 (1998).
- ²³H. Yan and G. U. Zhengbiao, "Morphology of Modified Starches Prepared by Different Methods," *Food Res. Int.*, **43** [3] 767–72 (2010).
- ²⁴M. H. Talou, M. A. Villar, and M. A. Camerucci, "Thermogelling Behavior of Starches to be Used in Ceramic Consolidation Processes," *Ceram. Int.*, **36** [3] 1017–26 (2010).
- ²⁵R. Barea, M. I. Osendi, P. Miranzo, and J. M. F. Ferreira, "Fabrication of Highly Porous Mullite Materials," *J. Am. Ceram. Soc.*, **88** [3] 777–9 (2005).
- ²⁶R. Moreno, J. S. Moya, and J. Requena, "Rheological Parameters of Mullite Aqueous Suspensions"; pp. 1053–61 in *Ceramics Today – Tomorrow's Ceramics: Proceedings of the 7th International Meeting on Modern Ceramics Technologies*. Montecatini Terme, Italy, 1991.
- ²⁷E. Gregorová, W. Pabst, and I. Boháčenko, "Characterization of Different Starch Types for Their Application in Ceramic Processing," *J. Eur. Ceram. Soc.*, **26** [8] 1301–9 (2006).
- ²⁸W. Pabst, E. Gregorová, I. Sedlářová, and M. Černý, "Preparation and Characterization of Porous Alumina-Zirconia Composite Ceramics," *J. Eur. Ceram. Soc.*, **31** [14] 2721–31 (2011).
- ²⁹L. B. Garrido, M. P. Albano, K. P. Plucknett, and L. Genova, "Effect of Starch Filler Content and Sintering Temperature on the Processing of Porous 3Y-ZrO₂ Ceramics," *J. Mater. Process. Technol.*, **209** [1] 590–8 (2009). □

Author Query Form

Journal: JACE
Article: 12852

Dear Author,



During the copy-editing of your paper, the following queries arose. Please respond to these by marking up your proofs with the necessary changes/additions. Please write your answers on the query sheet if there is insufficient space on the page proofs. Please write clearly and follow the conventions shown on the attached corrections sheet. If returning the proof by fax do not write too close to the paper's edge. Please remember that illegible mark-ups may delay publication.

Many thanks for your assistance.

Query reference	Query	Remarks
1	AUTHOR: As per the journal style, please limit the number of characters up to 30 in short title.	
2	AUTHOR: Please check that the title, author names, affiliations, and corresponding author information is listed accurately for publication.	
3	AUTHOR: Please define SEM.	
4	AUTHOR: Please define XRD.	
5	AUTHOR: Please give manufacturer information for X'Pert PRO, PANalytical: company name, town, state (if USA), and country.	
6	AUTHOR: Please provide the city name for Quantachrome Co.	
7	AUTHOR: Please provide the city name for Malvern Ltd.	
8	AUTHOR: Please provide city name for Avebe S.A.	
9	AUTHOR: Please give manufacturer information for IRAM 15040: company name, town, state (if USA), and country.	
10	AUTHOR: Please give manufacturer information for Shimadzu TGA-50: company name, town, state (if USA), and country.	
11	AUTHOR: Please give manufacturer information for Shimadzu DSC-50: company name, town, state (if USA), and country.	
12	AUTHOR: Please provide city name for Jeol JSM-6460.	
13	AUTHOR: Please give manufacturer information for Leica DMLB: company name, town, state (if USA), and country.	
14	AUTHOR: Please give manufacturer information for Linkam THMS 600: company name, town, state (if USA), and country.	
15	AUTHOR: Please give manufacturer information for Leica DC 100: company name, town, state (if USA), and country.	
16	AUTHOR: Please provide city name for Zschimmer & Schwarz.	
17	AUTHOR: Please provide city name for Thermo Electron Corp.	
18	AUTHOR: Please provide city name for Thermo Haake.	
19	AUTHOR: Please give manufacturer information for Memmert UFP 400: company name, town, state (if USA), and country.	
20	AUTHOR: Please provide city name for Carbolite Ltd..	
21	AUTHOR: Please give manufacturer information for slide caliper: company name, town, state (if USA), and country.	
22	AUTHOR: Please provide city name for Micromeritics.	
23	AUTHOR: Figure 9 has not been mentioned in the text. Please cite the figure in the relevant place in the text.	

Proof Correction Marks

Please correct and return your proofs using the proof correction marks below. For a more detailed look at using these marks please reference the most recent edition of The Chicago Manual of Style and visit them on the Web at: <http://www.chicagomanualofstyle.org/home.html>

<i>Instruction to typesetter</i>	<i>Textual mark</i>	<i>Marginal mark</i>
Leave unchanged	... under matter to remain	<u>stet</u>
Insert in text the matter indicated in the margin	^	^ followed by new matter
Delete	Ʒ through single character, rule or underline or Ʒ through all characters to be deleted	Ʒ
Substitute character or substitute part of one or more word(s)	Ƶ through letter or — through characters	new character Ƶ or new characters Ƶ
Change to italics	— under matter to be changed	<u>ital</u>
Change to capitals	≡ under matter to be changed	<u>Caps</u>
Change to small capitals	≡ under matter to be changed	<u>sc</u>
Change to bold type	~ under matter to be changed	<u>bf</u>
Change to bold italic	~ under matter to be changed	<u>bf+ital</u>
Change to lower case	Ɔ	<u>lc</u>
Insert superscript	√	√ under character e.g. √
Insert subscript	^	^ over character e.g. ^
Insert full stop	⊙	⊙
Insert comma	↵	↵
Insert single quotation marks	↵ ↵	↵ ↵
Insert double quotation marks	↵ ↵	↵ ↵
Insert hyphen	=	=
Start new paragraph	¶	¶
Transpose	┌┐	┌┐
Close up	linking  characters	
Insert or substitute space between characters or words	#	#
Reduce space between characters or words	˘	˘